# Calorimeters for Cosmic Rays

J. F. Ormes and J. F. Arens
Goddard Space Flight Center
Greenbelt, Maryland 20771

Calorimeters are useful devices in balloon borne and satellite cosmic ray experiments because of their large dynamic energy range and, for some applications, their good spatial and energy resolution. Energy spectra of electrons, protons, and heavier ions have been measured. Special applications of calorimeters include gamma ray spectroscopy and accurate energy determinations for isotope spectroscopy.

---

Calorimeters were first used in mountain top studies of cosmic ray atmospheric secondaries in late 1950's (N. L. Grigorov, 1958). During the late 1960's, these devices were first carried above the atmosphere to make direct observations of cosmic ray particles from satellites (Grigorov, 1970) and balloons (Jones et al., 1969). It is the use of these devices to make measurements of the spectra and composition of the cosmic rays that is the subject of this paper.

First, let us describe a few of the characteristics of the cosmic radiation we wish to observe. Of primary importance is the fact that cosmic rays include both electrons and nuclei from protons to iron. A typical observed nuclear abundance distribution is shown in Figure 1. Elements up to lead and uranium are also present, but so far calorimetric techniques have not been applied to these heavier nuclei. Observed differential spectra of electrons and nuclei are shown in Figure 2. These spectra are in general described by power laws $dN/dE = kE^{-\gamma}$, with exponents varying from $\gamma = 2.2 \pm 0.2$ for iron nuclei up to $\gamma = 2.75 \pm 0.05$ for protons and possibly as steep as $\gamma = 3.4 \pm 0.2$ for electrons. Measurements of the shapes of these spectra are of interest in determining the acceleration and energy loss mechanisms. For example, the electrons are expected to lose energy due to synchrotron radiation and to inverse compton collisions with the blackbody radiation which has cooled down to its current 3°K value as the universe expanded. This should cause the spectrum to steepen by $\Delta\gamma = 0.5$ or 1 depending upon the propagation model. While various workers have measured various spectral exponents from 2.7 to 3.4 between 10 and 1000 GeV, no one has been able to measure a changing spectral exponent within the energy range of his experiment.

Other important recent observations of cosmic ray spectra include the following: (1) the proton and helium spectra are similar in rigidity (Webber and Lezniak, 1975) rather than in energy/amu, (2) the spectra of secondary nuclei (Li, Be, B, N, $17 \leq Z \leq 24$) have spectra steeper than their primary progenitors by $\Delta\gamma \approx 0.3$ (Smith et al., 1973), and (3) the suggestion that the spectrum of iron nuclei is flatter than that of the other primary nuclei by perhaps as much as $\Delta\gamma = 0.5$ (Ormes and Balasubrahmanyan, 1973, and Juliusson, 1974). In all of these cases cosmic ray calorimeter measurements have played an important role (Ryan et al., 1972).

The respective implications of these results are (1) that cosmic ray acceleration is a magnetic rather than an electric process, (2) that the escape of the particles from a storage region, either in the source or in the galaxy is weakly energy (or rigidity) dependent and (3) that the iron spectrum may be too flat to be explained as a propagation effect. A sample (the selection effect being the ease of obtaining a figure easy to reproduce) of the calorimeters that have been flown on balloons are shown in Figures 3 (Balasubrahmanyan and Ormes, 1974) and 4 (Meegan and Earl, 1975). These experiments studied the nuclear and the electron components respectively. A totally active calorimeter for measuring gamma ray energies between 10 to 100 MeV is shown in Figure 5 (Hofstadter and Fichtel, 1974).

Since the electron steepening (and other astrophysical phenomena postulated) are expected to take place over a decade in energy, it is extremely important to measure spectra over large dynamic ranges with the same instrument. The calorimeter or ionization spectrometer as we have called it is the ideal instrument to make these measurements. It can be designed to have nearly constant resolution over a large dynamic range and it has no intrinsic upper limit.

There are very different considerations involved in the design of calorimeters for cosmic ray studies. First, the incident beams are isotropic, and second the spectra are steeply falling. And so for any balloon or satellite exposure the geometric collection factor of the payload must be optimized while the weight is minimized. This can be done by appropriate selection of materials. For a detector of uniform cross sectional area, a, and length, L, the geometrical factor, GF, is given by

$$GF \approx a^2/L^2 \text{ (for } L^2 \gg a\text{)}.$$

This can be expressed in terms of the weight, W, to which the detector is constrained and the properties of the detector material: the length T of the detector in gm/cm$^2$ and the mean density, $\rho$, in gm/cm$^3$. Since $a = W/T$ and $L = T/\rho$,

$$GF \propto \frac{W^2 \rho^2}{T^4} .$$

Since the weight is independently constrained, the geometrical factor is optimized by choosing the material with the largest $\rho^2/T^4$.

For any particular detector material, the desired energy resolution fixes the minimum acceptable T. The energy resolution is determined by two types of fluctuations in the signal output from the active layers of the ionization spectrometers: in the fraction of energy going into nuclear disintegrations and in the energy escaping through the bottom. The percentage fluctuations are smaller, the larger the number of nuclear interactions lengths along the path of the incident particle.

Both the column density ($gm/cm^2$) per interaction length and the number of interaction lengths necessary to achieve a particular energy resolution vary with detector material. The value of $\lambda$ increases slowly with atomic number, favoring absorbers of low atomic number. On the other hand, because the inelasticity increases in heavier materials and the radiation length decreases, the number of interaction lengths necessary to achieve a particular energy resolution decreases with increasing atomic number (W. V. Jones, 1969). These two effects tend to cancel and as a result, the column density necessary to achieve a given energy resolution is only weakly dependent on the detector material. For example, it increases by less than 25% from iron to tungsten.

The optimization depends mainly on the density. Since the scintillator layers tend to reduce the density, the number of samplings should be no more than is necessary to achieve an energy resolution consistent with the performance of the rest of the instrument. Samplings each 4 $X_0$ in 5$\lambda$ of tungsten gives $\sim$ 20% energy resolution for 100 GeV protons. The resolution is better by about a factor of two for $\alpha$-particles and should improve even more for heavier nuclei.

The geometrical factors, calculated for three different absorber materials for the allotted weight and for fixed energy resolution, are shown in Table I. The best choice for optimizing the geometrical factor is tungsten because of its extremely high density. However the dilution of the scintillators reduces the gain considerably. Tungsten has an additional advantage over iron (copper is slightly better than iron) because of its large ratio $\lambda/X_0$.

Under the severe layload constraints of space flight, the weight in the spectrometer should be utilized as effectively as possible. A variety of sampling scintillator arrangements have been suggested to optimize use of the detector surface. It has been found, however, that for payloads in the 2500-3000 kg class, so much of the weight is tied up in support structure, gondola, charge detectors, etc., that more imaginative geometries cannot be utilized. Gravity orientation away

Table I

COMPARISON OF GEOMETRICAL FACTORS FOR DIFFERENT MATERIALS

| Absorber Material | N[a] | $\lambda$ gm-cm$^{-2}$ | $\rho$ gm-cm$^{-3}$ | $\rho_{eff}$[b] gm-cm$^{-3}$ | Relative Geometrical Factor |
|---|---|---|---|---|---|
| Tungsten | 5 | 189 | 19.3 | 13.0 | 1.0 |
| Iron | 6 | 127 | 7.9 | 7.4 | 0.82 |
| Glass | 7 | 100 | 2.5 | 2.5 | 0.13 |

[a]Approximate number of nuclear interaction lengths needed to achieve less than 20% fluctuations for 100 GeV incident protons.

[b]The effective density of spectrometer plus sampling layers assuming one sample every 4 radiation lengths.

---

from the earth either by suspension from a balloon or on a gravity gradient stabilized platform optimizes the viewing time.

Future possibilities for development include optimization using poorer resolution thin spectrometers. Since calibration is possible now at 200 to 400 GeV, designs based upon Monte Carlo simulations can give both the shape of the fluctuation distribution and the energy dependence of energy loss effects. Knowing these things, energy spectra can be reconstructed even using 2.5 or 3 $\lambda$ thick spectrometers for protons and possibly even thinner for heavy nuclei. The energy resolution for protons calculated for one such device is shown in Figure 6. For heavy nuclei, which have large cross sections, even thinner spectrometers can be used. In Figure 7, we show the response of a calorimeter of different depths to heavy nuclei (Balasubrahmanyan, 1973; each module is 1/2 $\lambda$ thick).

As an amusing side light to a calorimeter conference, we wanted to close by showing a plastic scintillator calorimeter we have used to study cosmic ray isotopes. It works in an energy-range mode and a Cerenkov-range mode. It is shown in Figure 8 (Fisher et al., 1973). In Figure 9 is a histogram of the beryllium isotopes. $^{10}$Be has a half life of 1.5x10$^6$ years and is ideal for dating the cosmic rays. From this experiment we have obtained an age for the cosmic rays against leakage out of the galaxy of about 3x10$^6$ years which suggests that they spend most of their lifetime in regions of density about 1 atom/cm$^3$. This tends to suggest that cosmic rays at earth come from within a few kiloparsec of earth. Towards the galactic center the densities are higher, and away from the galactic plane, densities are lower.

## References


Balasubrahmanyan, unpublished (1973).

Balasubrahmanyan, V. K. and Ormes, J. F. Ap. J. 186, 109, (1974).

Fisher et al., Proc. XIII Intl. Conf. on Cosmic Rays, 4, 2895, (1973).

Grigorov, N. L., Murzin, V. S., Rappaport, I. D. JETP 34, 506, 1958.

Grigorov et al., Proc. XI Int. Conf. Cosmic Rays, Acta Phys., Suppl. No. 1, 29, 518, (1970).

Hagen et al., to be published.

Hofstadter and Fichtel, Explorer Gamma Ray Experiment Telescope, a proposal, May 1974.

Jones et al., Nucl. Inst. and Meth. 72, 173, (1969).

Jones, W. V., Phys. Rev. 187, 1868, (1969).

Juliusson, E., Ap. J., 191, 331, (1974).

Meegan and Earl, Ap. J. 197, 219, (1975).

Ormes and Balasubrahmanyan, Nature Phys. Sci., 241, 95, (1973).

Ryan et al., Phys. Rev. Lett., 28, 985, (1972).

Smith et al., Ap. J., 180, 987, (1973).

Webber, W. H. and Lezniak, J. A., Ap. and Space Sci., 30, 361, (1975).

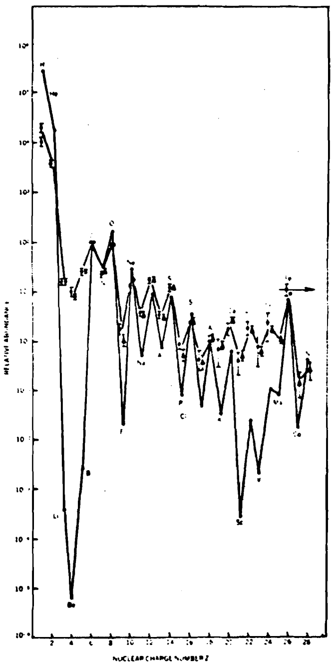

Fig. 1 (left) Relative abundance of the cosmic ray nuclei (carbon = 100), compared with the relative abundance of solar system elements.

Fig. 2 (below) On the left the data points are cosmic ray electron measurements; and the curve represents the proton spectrum. On the right the spectra of nuclei are given. Different curves represent different levels of solar modulation. Much of this high energy data comes from calorimeter measurements.

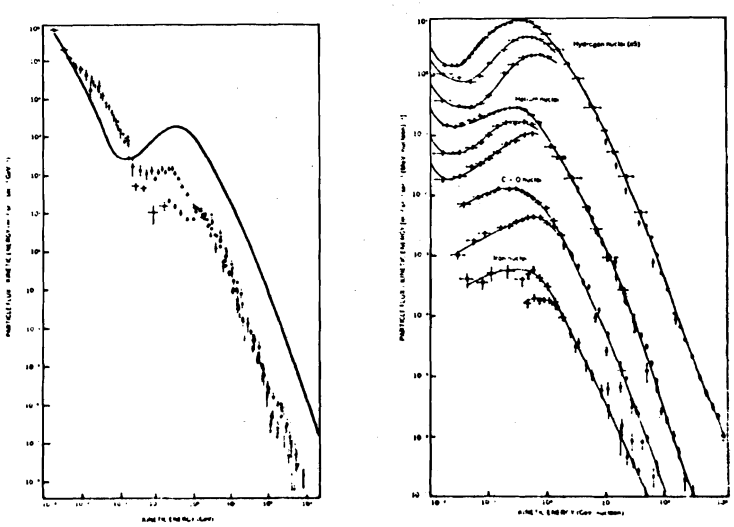

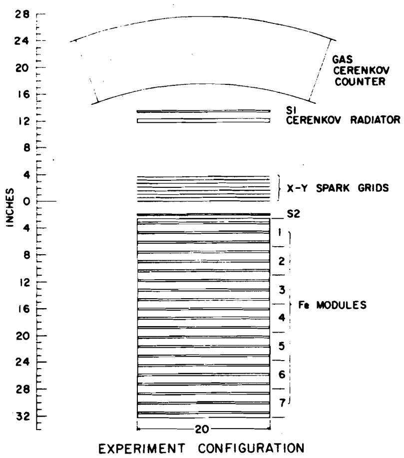


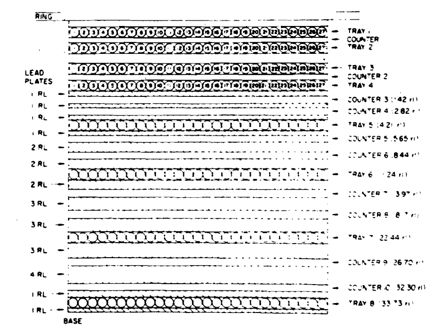


Fig. 3 Cosmic ray nuclear calorimeter experiment with a gas Cerenkov detector with 15 GeV/amu threshold. Each $\lambda/2$ module contains 3 scintillators.

Fig. 4 Cosmic ray electron calorimeter with a Geiger tube hodoscope.

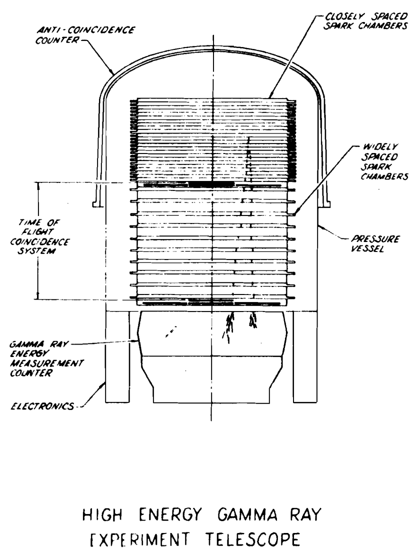


Fig. 5 Proposed satellite (EGRET) gamma ray telescope with CsI calorimeter

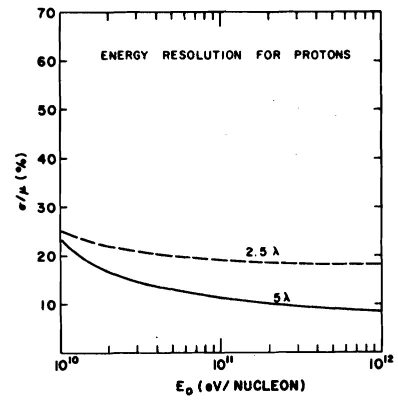


Fig. 6 Resolution versus energy for a tungsten spectrometer of 2 different depths.

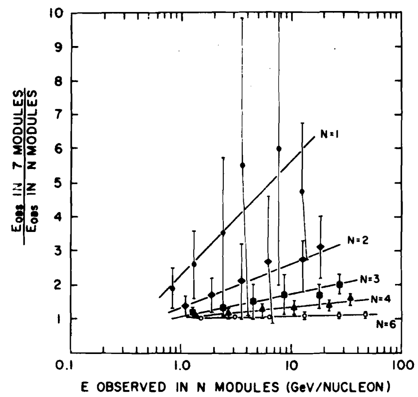


Fig. 7 Energy observed at different depths in iron spectrometer for heavy nuclei.

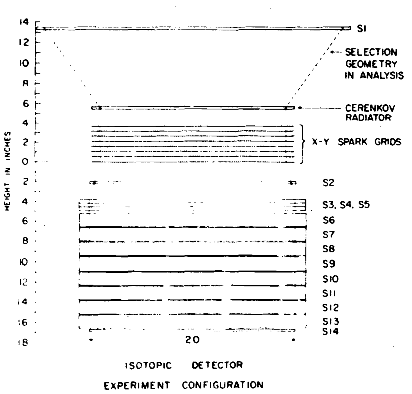


Fig. 8 Totally active plastic scintillator calorimeter for isotope measurements.

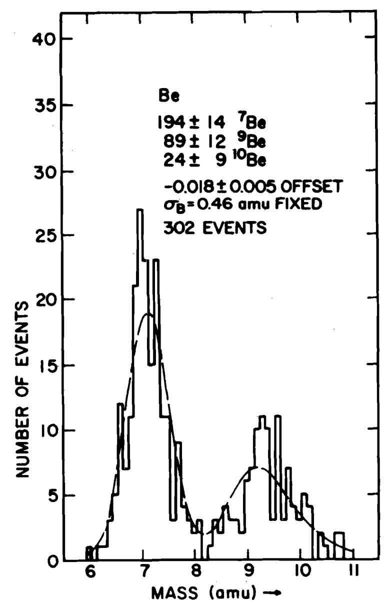


Fig. 9 Beryllium mass histogram from isotope calorimeter.